



Cite this: *RSC Adv.*, 2023, **13**, 1267

A more accurate indicator to evaluate oxidative stress in rat plasma with osteoporosis[†]

Wei-Chong Dong,^{‡ab} Jia-Liang Guo,^{‡c} Xin-Hui Jiang,^d Lei Xu,^e Huan Wang,^b Xiao-yu Ni,^b Ying-Ze Zhang,^{*c} Zhi-Qing Zhang^{*a} and Ye Jiang 

Background: oxidative stress is linked to various human diseases which developed into the idea of “disrupted redox signaling”. Osteoporosis (OP) is a chronic skeletal disorder characterized by low bone mineral density and deterioration of bone microarchitecture among which estrogen deficiency is the main cause. Lack of estrogen leads to the imbalance between oxidation and anti-oxidation in patients, and oxidative stress is an important link in the pathogenesis of OP. The ratio of the reduced to the oxidized thiols can characterize the redox status. However, few methods have been reported for the simultaneous determination of reduced forms and their oxidized forms of thiols in plasma. **Methods:** we developed a hollow fiber centrifugal ultrafiltration (HFCF-UF) method for sample preparation and validated a high-performance liquid chromatography tandem mass spectrometry (HPLC-MS/MS) method to determine two reduced forms of thiols-homocysteine (Hcy), cysteine (Cys) levels and their respective oxidized compounds, homocystine (HHcy) and cystine (Cyss) in rat plasma simultaneously for the first time. Thirty-six female rats were randomly divided into three groups: normal control (NC), oxidative stress (ovariectomy, OVX) and ovariectomy with hydrogen-rich saline administration (OVX + HRS). **Results:** the validation parameters for the methodological results were within the acceptance criteria. There were both significant differences of Hcy/HHcy (Hcy reduced/oxidized) and Cys/Cyss (Cys reduced/oxidized) in rat plasma between three groups with both $p < 0.05$ and meanwhile, the p values of malondialdehyde, superoxide dismutase and glutathione peroxidase were all less than 0.01. The value of both Hcy/HHcy and Cys/Cyss were significantly decreased with the change of Micro-CT scan result of femoral neck in OVX group (both the trabecular thickness and trabecular number significantly decreased with a significant increase of trabecular separation) which demonstrate OP occurs. The change of Hcy/HHcy is more obvious and prominent than Cys/Cyss. **Conclusions:** the Hcy/HHcy and Cys/Cyss could be suitable biomarkers for oxidative stress and especially Hcy/HHcy is more sensitive. The developed method is simple and accurate. It can be easily applied in clinical research to further evaluate the oxidative stress indicator for disease risk factors.

Received 5th September 2022
 Accepted 8th December 2022

DOI: 10.1039/d2ra05572d
rsc.li/rsc-advances

^aDepartment of Pharmacy, The Second Hospital of Hebei Medical University, 215# Heping West Road, Shijiazhuang, Hebei Province 050051, China. E-mail: 842178994@qq.com

^bDepartment of Pharmaceutical Analysis, School of Pharmacy, Hebei Medical University, 361# East Zhongshan Road, Shijiazhuang, Hebei Province 050017, China. E-mail: jiangle@hebmu.edu.cn

^cDepartment of Orthopaedics, The Third Hospital of Hebei Medical University, 139# Ziqiang Road, Shijiazhuang, Hebei Province 050000, China. E-mail: yzling_liu@163.com

^dDepartment of Obstetrics and Gynecology, Aerospace Central Hospital, Beijing 100049, China

^eDepartment of Neurology, The Second Hospital of Hebei Medical University, Shijiazhuang, Hebei Province 050051, China

[†] Electronic supplementary information (ESI) available. See DOI: <https://doi.org/10.1039/d2ra05572d>

[‡] Wei-Chong Dong and Jia-Liang Guo contributed equally to this work.

1 Introduction

For over three decades, ill health has been associated with the oxidative stress concept in the form of “an imbalance between oxidants and antioxidants in favor of the oxidants”, which developed into the idea of “disrupted redox signaling”.^{1,2} Increasing evidence suggests that oxidative stress is linked to various human diseases.³⁻⁵

Osteoporosis (OP) is a chronic skeletal disorder characterized by low bone mineral density and deterioration of bone microarchitecture, leading to increased risk in bone fragility and the susceptibility to occurrence of osteoporotic fracture.^{6,7} The prevalence of OP showed a tremendously increase and affected approximately one in three women and one in five men over the age of 50 years worldwide.⁸ OP is mainly divided into primary OP and secondary OP. The most common secondary OP is postmenopausal OP, a disease with high incidence and high



harmfulness, among which estrogen deficiency is the main cause.⁹

Lack of estrogen leads to the imbalance between oxidation and anti-oxidation in patients, and the oxidative stress level continues to rise, which induces inflammation and lipid peroxidation, resulting in cytotoxicity and harm to body health.¹⁰ Studies have shown that oxidative stress is an important link in the pathogenesis of OP in patients.^{11,12}

There are many indicators to assess oxidative stress, such as malondialdehyde (MDA), superoxide dismutase (SOD) and glutathione peroxidase (GSH-PX) and so on. Intracellular biotinols play a crucial role in combating oxidative stress and maintaining redox homeostasis by regulating the redox status between the reduced thiols and their oxidized disulfides.^{13,14} The determination of thiols and disulfides in plasma can provide valuable information to signal oxidative stress and has attracted extensive interest in recent years.^{15,16}

Homocysteine (Hcy) is a thiol amino acid resulting from the methylation of methionine, an essential amino-derived acid from dietary proteins (Fig. 1).¹⁷ Numerous clinical studies have concluded that Hcy is an independent risk factor for cardiovascular diseases.^{18–20} Hcy may be catabolized to cysteine (Cys) or remethylated to methionine.¹⁷ Cys contains free sulfhydryl groups with antioxidant activity and thus may be used to treat Cys storage disease and radiation damage.^{21,22}

Emerging evidence have also suggested the possible role of Hcy involving in bone, in which Hcy could affect bone tissue formation through disturbing the formation of collagen cross-links and normal calcification process, as well as reducing

bone blood flow.^{23,24} In the past two decades, there were extensive studies that have highlighted the linkages between aberrant Hcy concentrations with bone mineral density and osteoporotic fracture risk. Several investigations have shown the associations of hyperhomocysteinemia or increased Hcy levels with reduced bone mineral density and increased risk for osteoporotic fracture.^{25,26} However, there was some evidence that reported the inconsistent findings, in which there were no associations between the elevated levels of Hcy and bone mineral density.^{27,28} These contradictory results may be attributed to various confounders and the methodological limitations of conventional observational studies.⁸

There are many methods currently available for measuring plasma aminothiols.^{29–32} The total plasma concentration is mostly measured as an important element in clinical diagnostic evaluations.^{33–35} However, total thiols are the sum of free and protein-bound thiols and disulfides (derived from autoxidation of thiols).^{32–36} In fact, there is a state of dynamic equilibrium between their own oxidized and reduced thiols in the aminothiols. The ratio of the reduced to the oxidized thiols can characterize the redox status.^{33–39} Perturbation of plasma redox status and tissue aminothiol levels is an important indicator of chronic oxidative stress.³⁶ It has been reported that aminothiol concentration disturbances can also correspond to metabolic disorders, and the ratio of reduced and oxidized thiols indicates the redox state in the internal environment.^{36–39}

Many researchers have attempted to develop a simple and accurate method to simultaneously determine the reduced and oxidized thiols in biological fluids. However, these methods

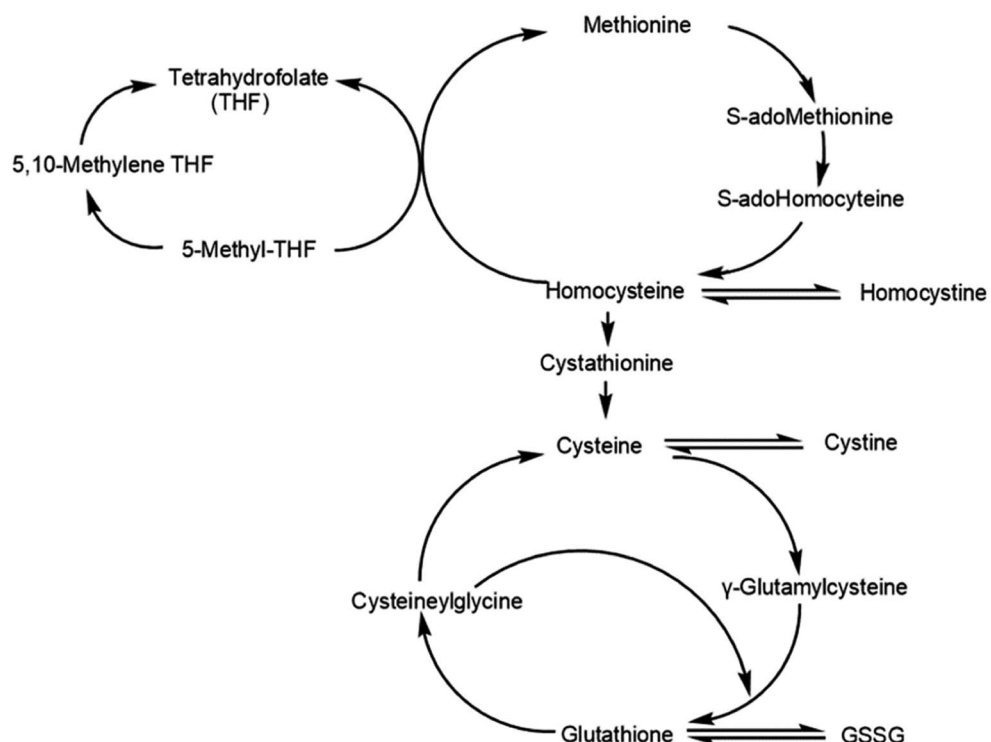


Fig. 1 Metabolic relation among aminothiols including the anabolic homocysteine remethylation pathway and the catabolic homocysteine transulfuration pathway (GSSG, oxidized glutathione).



suffer from several problems.^{13,34} The relatively low concentration in plasma (especially the very low concentration of oxidized thiols), as well as the poor traditional assay method sensitivity, has presented a major challenge in accurate and precise physiological concentration quantitation in clinical research.^{36–40} A formula for quantifying disulfides is based on thiols after and before reduction⁴¹ or indirectly calculated from the difference between the measurements obtained in the two separate steps.⁴² However, these methods, along with sequential thiols and disulfides detection, are time-consuming and vulnerable to thiol autoxidation, lowering result accuracy.¹³ The influence of enzymes on the oxidation equilibrium system was also not considered.

It has also been reported that different sample handling procedures for the same sample could lead to different reduced and oxidized thiol ratios.⁴³ Therefore, sample preparation plays a key role in aminothiol concentrations analysis in biological matrices. The protein precipitation (PPT) method has conventionally been used for measuring aminothiol in biofluids.^{33,39,44–46} While straightforward, the PPT method suffers from some drawbacks that may limit the accurate aminothiol measurement. It has poor analytical sensitivity and requires adding two to four times the volume of precipitation reagent into the sample. The operation was carried out in an open system without considering the influence of the environment on the redox system. Moreover, analyte coprecipitation with occlusion in the protein pellet may occur, leading to a low extract recovery rate and poor precision. The experimenters must be well trained, and even so, the recovery rate was only $75 \pm 18\%$.³⁹ Perchloric acid has been used as a protein precipitation reagent for aminothiol determination. However, perchloric acid is a strong oxidizing acid that may disturb the redox status balance, but it has not been discussed in the literature.^{15,39,45,46} The addition of perchloric acid changes the pH of the system and causes changes in the secondary structure of proteins, which may destroy enzymes *in vivo* and affect the balance of redox. In addition, unprecipitated proteins may affect the amount of free and protein-bound thiols and induce inaccurate measurements.⁴⁷ Solid-phase extraction (SPE)⁴⁴ or liquid–liquid extraction^{43,48} can improve the sensitivity and have cleaner pretreatment steps. However, the procedure is cumbersome and requires a long operation time in the open sample environment, which is particularly unadvisable because it can disrupt stability. Commercial centrifugal ultrafiltration (CF-UF) devices have been used for the quantitative analyses of aminothiol in blood samples, which only require a centrifugation step.^{34,43} A pressure gradient is applied to force the plasma aqueous components containing free drug molecules through a selective permeable membrane. However, the volume ratio of ultrafiltrate to sample solution is large and cannot be well controlled, especially for analyzing clinical samples with different plasma conditions, which affects the accurate analysis of drug concentrations with CF-UF.^{49–52}

Increasing analytical sensitivity and decreasing the influence of coprecipitation, strong oxidizing reagents, and unprecipitated proteins, especially, avoiding the effects of environmental changes on balance of redox *in vivo* are key to more accurate and

precise reduced and oxidized aminothiol concentration measurements. Fortunately, in this study, we developed a hollow fiber centrifugal ultrafiltration (HFCF-UF) device to avoid these influences.^{53,54} The sample preparation process was simplified to a 5 min centrifugation step without additional precipitation reagent. The sample macromolecules were completely intercepted by hollow fibers to reduce the interference with serum endogenous substances. The whole operation was carried out in a closed system, and the volume ratio of ultrafiltrate to sample solution was very small, which almost does not destroy the initial physiological state and the balance of redox system *in vivo*, and the result was more accurate.^{49,55}

In present work, the Sprague-Dawley (SD) rat with ovariectomy was chosen as the oxidative stress model with post-menopausal OP, and the hydrogen-rich saline was antioxidant.^{56–58} We aimed to develop a simple and accurate HFCF-UF method for fast and simultaneous determination of homocysteine (Hcy, reduced Hcy), cysteine (Cys, reduced Cys) and their own oxidized aminothiol, homocysteine (HHcy, oxidized Hcy), and cystine (Cyss, oxidized Cys) in rat plasma in order to evaluate the redox status.

2 Experimental

2.1 Chemicals and materials

Homocysteine (Hcy), homocystine, cysteine (Cys) and cystine were purchased from the Yuanye Bio-Technology Co., Ltd (Shanghai, China). The internal standard DL-homocysteine-D₄ (No. H591297) was obtained from Toronto Research Chemicals (Toronto, Canada). The blank rat plasma was offered from the Third Hospital of Hebei Medical University. *N*-ethylmaleimide (NEM) were obtained from Macklin Biochemical Co., Ltd (Shanghai, China) and formic acid (HPLC-grade) was purchased from Aladdin Biochemical Technology Co., Ltd (Shanghai, China). Acetonitrile (HPLC-grade) was purchased from Fisher Chemical (Lake Forest, CA). The deionized water was prepared by a Milli-Q50 water purification system (Millipore, Bedford, MA). All other chemical agents used were from analytical grade or HPLC grade. Hydrogen-rich saline (HRS, H₂ concentration >1.6 ppm) was provided by Beijing Hydrovita Beverage Co., Ltd. (Beijing, China) and stored under atmospheric pressure at 23 ± 2 °C in an aluminum pot with no dead volume.

The HFCF-UF devices were purchased from Hebei Heping Medical Equipment Factory (Shijiazhuang, China). The molecular cut-off was 10 kDa. The wall thickness of hollow fiber was 150 μm and the inner diameter was 1000 μm . The slim glass tubes were 7 cm of height and 3.5 mm of inner diameter.

2.2 Apparatus and instruments

A LC-20AD high-performance liquid chromatography (Shimadzu, Japan) system coupled to an API 4000⁺ (AB SCIEX, Los Angeles, CA, USA). Triple quadrupole mass spectrometer equipped were used for chromatographic analysis. Data were collected and analyzed using Analyst® version 1.6 software (AB SCIEX, Los Angeles, CA, USA). The R18 centrifuge Baiyang (Beijing, China) and CPA225D electronic analytical balance

(Germany, Sartorius) were used. XW-80 Vortex mixer (Shanghai Medical University Instrument Co., Shanghai, China) was also employed.

2.3 HPLC-MS/MS conditions

The chromatographic separation was achieved using an XAqua CN (4.6 × 150 mm, 5 μ m) column (Acchrom Technologies Co., Ltd, China), thermostated at 40 °C. The mobile phase consisted of solvent A (0.1% formic acid) and solvent B (acetonitrile, 0.1% formic acid) under an isocratic elution (95 : 5, v/v) at a flow rate of 0.8 mL min⁻¹. The injection volume was 10 μ L.

The compounds were detected with an electrospray ionization source operating in positive ion mode. The measuring parameters of the mass spectrometer were set as follows: ion spray voltage = 5500 V; temperature = 550 °C; source gas 1 = 55 psi; source gas 2 = 50 psi, and curtain gas = 40 psi, collision gas = 4 psi. Mass spectrometric detection was carried out by multiple reaction monitoring—employing the acquisition parameters summarized in Table 1.

2.4 Solution preparation

Individual stock solutions of Hcy (reduced), homocystine (HHcy, oxidized Hcy), Cys (reduced) and cystine (Cys, oxidized Cys) at a concentration of 5 mmol L⁻¹ and the internal standard homocysteine-*D*₄ (Hcy-*D*₄) at a concentration of 1.44 mmol L⁻¹ were prepared in acidified deionized water (hydrochloric acid) and kept at -40 °C. Fresh NEM at a concentration of 100 mmol L⁻¹ was prepared in phosphate-buffered saline (10 mmol L⁻¹, pH 7.4). A mixed working solution of the analytes containing Hcy-NEM (250 μ M), homocystine (20 μ M), Cys-NEM (250 μ M), and cystine (100 μ M) was prepared in deionized water by mixing appropriate volumes of the abovementioned individual stock solutions at 10 mmol L⁻¹ NEM and kept at -40 °C. The internal working solution 72 μ mol L⁻¹ Hcy-*D*₄-NEM was prepared by diluting the internal standard stock solution and mixing it with NEM at 10 mmol L⁻¹.

Linear working solutions (475 μ L) were prepared in deionized water by diluting the mixed stock solutions spiked with 25 μ L of internal standard working solutions ranging in intervals of 0.1–10 μ mol L⁻¹ for Hcy-NEM and Cys-NEM, 0.04–4 μ mol L⁻¹ for cystine and 0.008–0.8 μ mol L⁻¹ for homocystine, containing internal standard Hcy-*D*₄-NEM at 3.6 μ mol L⁻¹.

Table 1 MRM conditions of thiols and internal standards

Analyte	Parent (m/z)	Daughter (m/z)	DP (V)	CE (eV)	D _{well} (ms)
Hcy-NEM	261.2	215.2	72	16	100
Homocystine	269.3	136.3	35	12	100
Cys-NEM	247.2	201.4	68	15	100
Cystine	241.3	152.2	40	18	100
Hcy- <i>D</i> ₄ -NEM	265.1	219.1	70	15	100

2.5 Sample preparation⁵⁹

Blood samples were collected in the sealed HFCF-UF device, as shown in Fig. 2, containing EDTA, 50 μ L internal working solution and 100 μ L of NEM reagent at a 100 mmol L⁻¹ concentration to avoid thiol autoxidation. Immediately, it was added to 900 μ L of whole blood sample, and the mixture was left to react for 1 min. Then, after a simple centrifugation at 2.40 × 10³ g for 5 min at 4 °C, the ultrafiltrate in the hollow fiber lumen was pushed out from the other end of the hollow fiber using a syringe. Thirty microliters of ultrafiltrate and 30 μ L of 2% sulfosalicylic acid were mixed, and 10 μ L was injected into the LC-MS/MS system for analysis.

2.6 Animal model and treatment

A total of 36 (12 animals per group) 12 weeks-old female SD rats (300 g ± 13 g) obtained from Hebei Medical University Animal Center were used in our study. The study was approved by the Ethics Board of the Third Hospital of Hebei Medical University and was conducted in accordance with the institutional guidelines for the care and treatment of rats. The female rats were kept in a stable ambient environment (temperature 24 ± 2 °C, humidity 45% to 55% and 12 hours light–dark cycle from 7 a.m. to 7 p.m., specific pathogen free) with free access to tap water and rodent chow diet. Changes in appearance were monitored and addressed immediately.

After one week acclimation period, Estrogen withdrawal was operated by ovariectomy (OVX) *via* a dorsal approach (one incision located at the middle back) in 24 SD rats. The other 12 female rats without OVX underwent sham surgeries with ovaries simply exposed were normally raised are the Normal Control group (NC). At 12 weeks after OVX operation, the 24 SD rats were then divided randomly into two group (*n* = 12). One group were received intragastric administration of normal saline (OVX). The other group were intragastric administration of HRS at 5 mL per day in the OVX + HRS group. After 4 weeks, the rats were anesthetized through intraperitoneal injections and then the femoral were prepared for Micro-CT scanning. The rats in all groups were euthanized by exsanguination *via* the abdominal aorta different observation periods under anesthesia. The rat blood was collected (about 4 mL) to EDTA anticoagulant tube from the abdominal aorta immediately prior to sacrifice.

3 Results

3.1 Nonspecific binding

A significant disadvantage in this procedure is drug nonspecific binding with filter membranes or glass and plastic devices. Therefore, nonspecific binding must be quantified first.⁵⁰ Two different hollow fiber materials, polysulfone and polyacrylonitrile, were chosen to evaluate the nonspecific binding. The ratios of the obtained concentrations from HFCF-UF to the corresponding standard concentrations at three (low, middle, high) concentrations of Hcy-NEM, homocystine, cysteine-NEM and cystine in phosphate-buffered saline were all approximately 100%, as well as the internal standard Hcy-*D*₄-NEM at 3.6 μ mol L⁻¹, as shown in ESI S1.† Thus, there was no significant

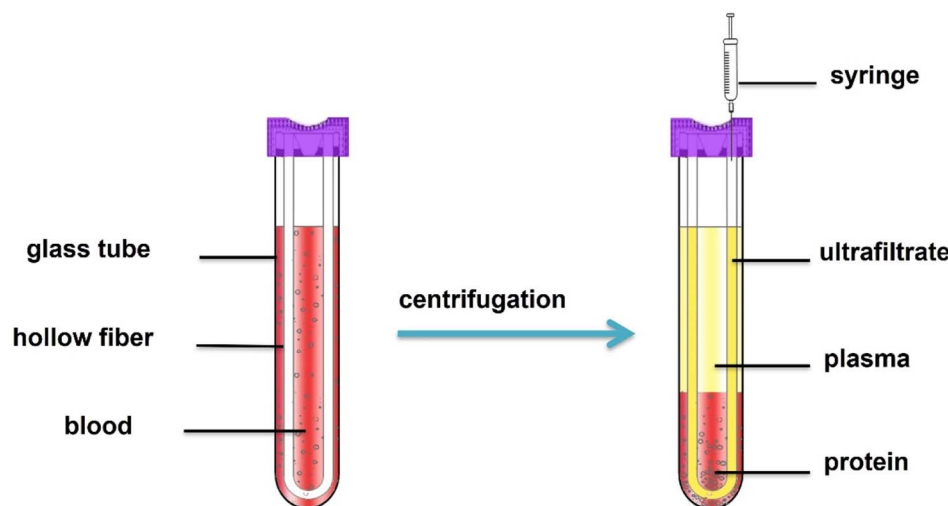


Fig. 2 Hollow fiber centrifugal ultrafiltration (HFCF-UF) device.

nonspecific binding, and these two kinds of hollow fibers could both be used in subsequent studies.

3.2 Method validation

3.2.1 Selectivity. The Hcy-NEM, Cys-NEM, cystine, homocystine, and internal standard retention times were 3.16, 2.91, 2.32, 2.49, and 3.16 min, respectively. Representative chromatograms of Hcy-NEM and homocystine in rat plasma samples are shown in Fig. 3 and others in ESI S2.†

3.2.2 Linearity, LOD and LOQ. The calibration curves were generated by plotting the analyte and the internal standard peak area ratios at different concentrations for linear regression analysis by a weighted factor $1/C^2$ (0.1, 0.2, 0.5, 1.0, 2.5, and 5 μM for Hcy-NEM and Cys-NEM; 0.04, 0.08, 0.2, 0.4, 1.0, and 2 μM for cystine; and 0.004, 0.008, 0.016, 0.04, 0.08, 0.2, and 0.4 μM for homocystine). The method provided adequate linearity for all the analytes within the corresponding concentration ranges. $Y_{\text{Hcy-NEM}} = 0.213C - 0.000431$ ($r^2 = 0.9997$), $Y_{\text{Cys-NEM}} = 0.236C + 0.00295$ ($r^2 = 0.9995$), $Y_{\text{cystine}} = 0.36C - 0.00087$ ($r^2 = 0.9989$), $Y_{\text{homocystine}} = 1.35C + 0.00149$ ($r^2 = 0.9937$). The limits of detection (LODs) and the limits of quantification (LOQs) were assessed by determining the lowest analyte concentrations that resulted in signal-to-noise ratios of ≥ 3 and ≥ 10 , respectively. The LOD and LOQ were 0.02 and 0.1 μM for both Hcy-NEM and Cys-NEM, 0.01 and 0.04 μM for cystine, and 0.002 and 0.04 μM for homocystine.

3.2.3 Accuracy, precision and matrix effects. The QC samples (low, middle, high) were prepared in deionized water by diluting the mixed stock solutions and then spiking them with 25 μL of internal standard working solutions. The intraday precision and relative recovery determination were conducted with five replicates of three QC sample concentrations on the same day. Interday precision was evaluated on 3 consecutive days. Extraction recovery was reported as the percent of measured concentrations (background subtraction) in spiked rat plasma samples prepared according to Section 2.5 relative to

the spiked concentrations in blank plasma ultrafiltrate. Matrix effects were also evaluated quantitatively by the blank plasma ultrafiltrate spike method, comparing measured analyte concentrations in plasma ultrafiltrate to concentrations in standard solution at three concentrations. Satisfactory results were obtained and are listed in Tables 2 and 3.

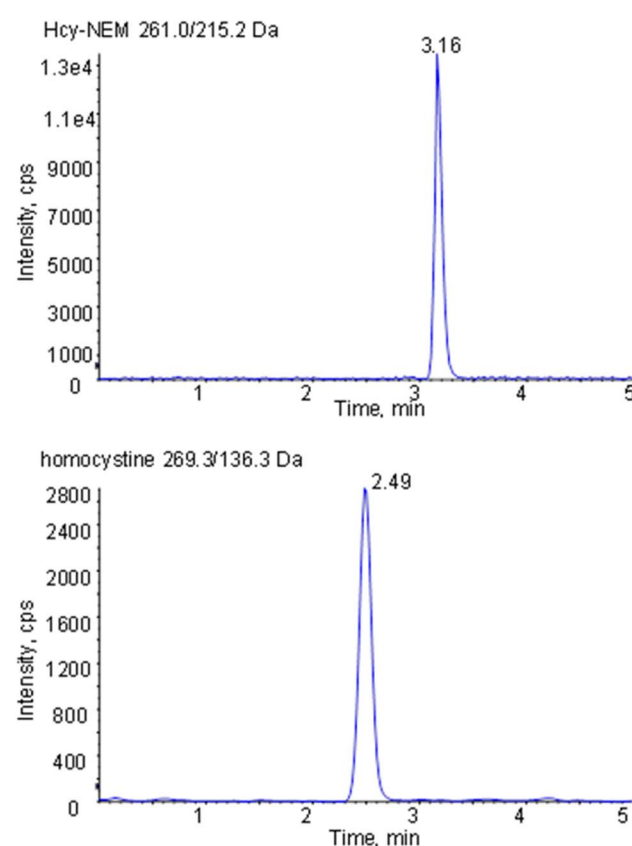


Fig. 3 Representative MRM chromatograms of Hcy-NEM and homocystine in rat plasma sample.

Table 2 Results of relative recovery and precisions test for the analysis of Hcy-NEM, Cys-NEM, cystine (Cyss) and homocystine (HHcy) in QC samples ($n = 5$)

Analyte	Spiked concentration ($\mu\text{mol L}^{-1}$)	Measured concentration ($\mu\text{mol L}^{-1}$)	Relative recovery (%)	Intra-RSD (%)	Inter-RSD (%)
Hcy-NEM	0.1	0.102	102	9.5	9.7
	1	0.955	95.5	2.8	5.3
	4	3.84	96.1	5.6	3.9
Cys-NEM	0.1	0.0956	95.6	7.0	8.1
	1	0.929	92.9	2.3	7.5
	4	3.67	91.7	8.1	5.7
Cystine	0.04	0.0453	113	2.4	5.9
	0.4	0.428	107	4.2	5.6
	1.6	1.40	87.7	4.7	4.8
Homocystine	0.008	0.00873	109	4.4	6.1
	0.08	0.0777	97.2	7.1	7.6
	0.32	0.295	92.1	4.7	4.1

3.2.4 Stability. We evaluated the room temperature stability, freezing stability and freeze-thaw stability as well as after-processing stability. QC samples at three concentrations (low, middle, high) maintained at room temperature (26 °C) for 12 h, after three freeze-thaw cycles, kept at –40 °C for 14 days, and set in the autosampler at 15 °C for up to 24 h after processing were all stable with RSD values below 13%, as shown in ESI S3.†

3.3 Application to rat blood samples

About 2 mL rat blood samples were collected to EDTA anticoagulant tube and centrifuged for 5 min at 2.4×10^3 g. And then, the obtained supernate plasma samples were used to measure MDA, SOD and GSH-PX following enzyme-linked immunosorbent assay kits reconstruction (Nanjing Jiancheng Institute of Biological Engineering). The MDA, SOD, and GSH-PX results were listed in Table 4. Another 1 mL rat blood samples were prepared according to Section 2.5 for the analysis of Hcy (reduced), HHcy (oxidized Hcy), Cys (reduced) and Cyss (oxidized Cys). The ratios of Hey/HHcy (Hey reduced/oxidized) and Cys/Cyss (Cys reduced/oxidized) were also calculated and shown in Fig. 4.

The region 7 mm proximal and distal (about 393 slices more or less) surrounding the femoral was set as the region of interest. The region of interest was selected on the two-dimensional CT images automatically. The trabecular thickness (Tb·Th, mm), trabecular number (Tb·N, 1/mm) and trabecular separation (Tb·Sp, mm) were recorded and calculated, as shown in Table 5. The representative Micro-CT scan images of femoral neck in three groups were shown in Fig. 5.

3.4 Statistical analysis

The statistical analysis was performed using the SPSS 24.0 statistical package, and the *P* values were calculated by one-way analysis of variance, as shown in Fig. 4, Tables 4 and 5. The values of *P* < 0.05 were considered to be statistically significant.

4 Discussions

4.1 Comparison with other methods

It has been reported that different sample handling procedures can also lead to different results of reduced and oxidized aminothiol ratios.⁴³ Thus, it is essential to develop a simple and accurate pretreatment method for analyzing reduced and oxidized thiols.

Table 3 Results of extraction recovery and matrix effects for the analysis of Hcy-NEM, Cys-NEM, cystine (Cyss) and homocystine (HHcy) in spiked samples ($n = 5$)

Analyte	Spiked concentration ($\mu\text{mol L}^{-1}$)	Measured concentration ($\mu\text{mol L}^{-1}$)	Extraction recovery (%)	Matrix effects (%)
Hcy-NEM	0.1	0.0877	95.6	100
	1	0.890	103	98.1
	4	4.06	97.5	108
Cys-NEM	0.1	0.108	102	104
	1	0.915	101	92.6
	4	4.40	101	106
Cystine	0.04	0.0436	94.3	108
	0.4	0.392	106	89.7
	0.8	0.838	98.6	104
Homocystine	0.004	0.00423	98.0	102
	0.04	0.0390	97.2	92.5
	0.32	0.3320	100.6	89.6



Table 4 Results of MDA, SOD, GSH-PX in 36 rats plasma samples in the three groups (NC: normal control, OVX: ovariectomy, OVX + HRS: ovariectomy with hydrogen-rich saline administration)

Group	MDA ($\mu\text{mol L}^{-1}$)	SOD (U mL^{-1})	GSH-PX ($\mu\text{mol L}^{-1}$)
NC	4.85 \pm 11.09	94.82 \pm 5.60	1892.69 \pm 393.37
OVX	6.41 \pm 1.12	77.99 \pm 4.51	1588.82 \pm 492.18
OVX + HRS	5.53 \pm 1.05 ^a	86.79 \pm 4.47 ^a	2127.87 \pm 263.82 ^a

^a The statistical analysis of three groups (NC, OVX, OVX + HRS) showed that $p < 0.01$.

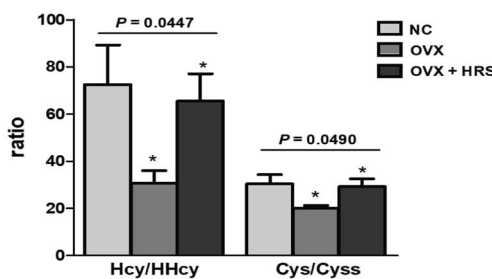


Fig. 4 The ratio of reduced to oxidized from (Hcy/HHcy and Cys/cystine) in rat plasma samples in three groups (NC: normal control, OVX: ovariectomy, OVX + HRS: ovariectomy with hydrogen-rich saline administration).

Table 5 Results of Micro-CT scan of femoral in 36 rats in the three groups (NC: normal control, OVX: ovariectomy, OVX + HRS: ovariectomy with hydrogen-rich saline administration)

Group	Tb·Th (mm)	Tb·N, (1/mm)	Tb·Sp (mm)
NC	112.92 \pm 5.72	6.57 \pm 0.75	0.19 \pm 0.059
OVX	92.46 \pm 9.12	4.98 \pm 0.74	0.32 \pm 0.061
OVX + HRS	102.22 \pm 7.14 ^a	5.55 \pm 0.76 ^a	0.25 \pm 0.043 ^a

^a The statistical analysis of three groups (Tb·Th, Tb·N, Tb·Sp) showed that $p < 0.001$.

Our team has reported a simple and accurate HFCF-UF method for the analysis of homocysteine, cysteine, cysteinyl-glycine, and glutathione in human blood, but it can not measure the

reduced and their respective oxidized compounds simultaneously.⁵⁹

HFCF-UF is a patent of State Intellectual Property Office, Project No. ZL 200910074429.4, which invented by our research group. It consists of a slim glass tube and a U-shaped hollow fiber, and it has been employed to separate the macromolecules from plasma or other complicated matrixes.^{49,51,53-55} Hollow fiber plays a physical interception role according to different molecular weight. At present, it has been commercialized by Hebei Heping Medical Equipment Factory (Shijiazhuang, China, Registration No: Jixin Equipment 20200013).

In this study, we developed a HFCF-UF method⁵³⁻⁵⁵ to separate homocysteine (Hcy), cysteine (Cys) levels and their respective oxidized compounds, homocystine (HHcy) and cystine (Cyss) from a complicated matrix for the first time to evaluate oxidative stress, and the results showed great merits. Without additional precipitation reagent, the sample was directly centrifuged, avoiding the problems of poor analytical sensitivity, coprecipitation, strong oxidizing acid, and unprecipitated proteins normally associated with the PPT method. Compared with LLE and SPE, the separation protocol was simplified to ordinary centrifugation for 5 min, and could be more suitable for routinely analyzing large amounts of clinical samples.⁴⁹ Moreover, with HFCF-UF, the volume ratio of ultrafiltrate to sample solution was not only small but could also be precisely controlled. The initial physiological state was almost not disturbed. Thus, the result was more accurate and precise than CF-UF.^{51,53,55} Furthermore, the macromolecules in the samples could be completely intercepted by hollow fibers to reduce endogenous substance disturbance in the blood samples and reduce matrix effects. Method validation results were excellent, with matrix effects less than 11% and extraction recovery of 94.3–103%. The intra-RSD and inter-RSD were all less than 10%. Especially, the whole operation was performed in a closed system which almost not disturb the redox equilibrium system *in vivo* and the results were more reliable.

Homocysteine (Hcy) and cysteine (Cys) are reduced aminothiols, and due to the high reactivity of the thiol group, which are easily transformed into its mixed and symmetrical disulfides (oxidized form).⁴⁴ Therefore, it is a key to stabilize thiol groups by immediate derivatization for accurate measurement.

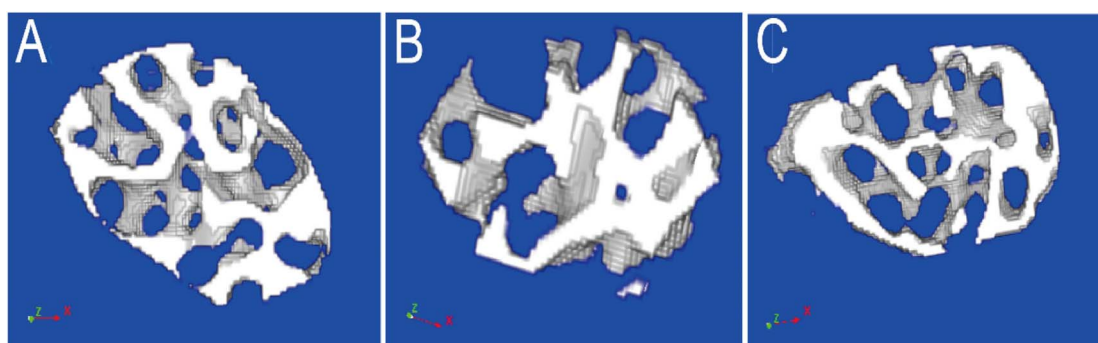


Fig. 5 The Micro-CT scan images of femoral neck in three groups ((A) NC, normal control, (B) OVX, ovariectomy, (C) OVX + HRS, ovariectomy with hydrogen-rich saline administration).



We have discussed the comparation of different derivatization reagents including *N*-(1-phenylethyl) maleimide, 2-vinyl-pyridine and NEM in our previous study.⁵⁹ The fast-reacting reagent, NEM may provide more accurate results. Therefore, we selected NEM as a suitable reagent in our present work.

4.2 Rat sample data analysis

We chose the ovariectomized rat as oxidative stress model with postmenopausal OP which was commonly reported in literature.⁵⁶ It has also reported that systemic delivery of hydrogen saline water may improve the reservation of bone tissue in the tibias and femurs of osteoporotic rats caused by diabetes mellitus, which was characterized by increased levels of oxidative stress and overproducing reactive oxygen species. In present work, the MDA increased and SOD, GSH-PX decrease significantly in OVX group which in line with the oxidative stress status as literature reported. In OVX + HRS group, the MDA decreased and SOD, GSH-PX increased to tended to normal control group. The statistical analysis of MDA, SOD and GSH-PX between three groups (NC, OVX, OVX + HRS) all showed that $p < 0.01$ in Table 4.

Usually, the value of Tb·Th and Tb·N decreased and Tb·Sp increased when osteoporosis occurs.⁶⁰ The Micro-CT scan of femoral in 36 rats in Table 5 and Fig. 5 showed that there were significant decrease of Tb·Th and Tb·N and a significant increase of Tb·Sp in OVX group, while the values were significantly improved and tended to normal group in OVX + HRS group with significant statistical differences of Tb·Th, Tb·N, Tb·Sp with $p < 0.001$. These results indicated that the oxidative stress model with postmenopausal OP was modeled successfully, and hydrogen water can effectively fight oxidative stress and treat postmenopausal OP as it reported in previous studies.⁵⁶

There were significant differences of Hcy/HHcy (Hcy reduced/oxidized) and Cys/Cyss (Cys reduced/oxidized) in rat blood between three groups with p value was 0.0447 and 0.049, respectively, as it shown in Fig. 4. The results were consistent with the results in Tables 4 and 5. Thus, the ratio of Hcy/HHcy and Cys/Cyss could be suitable biomarkers for oxidative stress. The value of Hcy/HHcy and Cys/Cyss decreases when oxidative stress occurs. It may be explained that the reduced forms of homocysteine, cysteine (Hcy, Cys) decrease, and the oxidized forms (HHcy, Cyss) increase with oxidative stress, which induce the decreases of the ratio (Hcy/HHcy, Cys/Cyss).

4.3 The sensitivity of Hcy/HHcy and Cys/Cyss

Oxidative stress and redox signaling involve electron transfer reactions, and E_h is a convenient parameter describing the relationship between various biochemicals undergoing oxidation-reduction reactions,^{61–63} as defined by the Nernst equation as below:

$$E_h = E_0 + \frac{RT}{nF} \ln \frac{[\text{oxidized}]}{[\text{reduced}]} \quad (1)$$

E_h depends on both the inherent chemical properties to accept or donate electrons, expressed in the standard potential

(E_0), and the coupled species acceptor (oxidized) and donor (reduced) concentrations, where R is the gas constant (8.313 J K⁻¹ mol⁻¹), T is the absolute temperature (K), n is the number of electrons transferred, and F is Faraday's constant.

If there is a change in the reduced to oxidized thiol ratio, there is a change in E_h , which signals oxidative stress.⁶² Therefore, the reduced and oxidized thiol ratio indicates the redox state in the internal environment.⁴⁴ Especially, the HHcy (oxidized) concentration was far lower than that of Hcy (reduced). Thus, a subtle oxidation change would lead to a significant change in the reduced to oxidized thiol ratio and further affect the E_h and signal oxidative stress. Therefore, accurate reduced and oxidized level measurement is key to evaluating oxidative stress.

Furthermore, we also founded that Hcy/HHcy (Hcy reduced/oxidized) is more sensitive than Cys/Cyss (Cys reduced/oxidized) with a more obvious and prominent change in Fig. 4. It maybe due to the concentrations of Cys and Cyss are both relatively high, and more than ten times higher than Hcy and HHcy, which is in line with the literature reported, as it shown in Table 6. The potential difference of $E_{\text{HHcy/Hcy}}$ after and before the redox reaction is $\Delta E_{\text{HHcy/Hcy}}$; the potential difference of $E_{\text{Cyss/Cys}}$ before and after the redox reactions is $\Delta E_{\text{Cyss/Cys}}$.

$$R = \frac{\Delta E_{\text{HHcy/Hcy}}}{\Delta E_{\text{Cyss/Cys}}} = \frac{\frac{RT}{nF} \ln \frac{5}{2}}{\frac{RT}{nF} \ln \frac{41}{38}} = 12.06 \quad (2)$$

From the eqn (2), we found that with a redox reaction *in vivo*, the change of $\Delta E_{\text{HHcy/Hcy}}$ is 12 times that of $\Delta E_{\text{Cyss/Cys}}$. The corresponding formula derivation process show in detail in ESI S4.† It indicated that the Hcy/HHcy is a more sensitive biomarker than Cys/Cyss for oxidative stress. The Hcy and HHcy were not involved in protein synthesis and a slight change in the Hcy/HHcy will result in a titration jump to signal oxidative stress.

4.4 Relationship of Hcy/HHcy and Cys/Cyss with osteoporosis

Some literature reported the contradictory results about the linkages between aberrant Hcy concentrations with bone mineral density and osteoporotic fracture risk.⁸ Several investigations have shown that increased Hcy level is associated with decreased bone mineral density and increased risk of fracture.^{24,25} Reports have shown that hyperhomocysteinemia has adverse effects on nerve cells, vascular endothelial cells, osteoblasts and osteoclasts. The increase of Hcy concentrations increases the level of oxidative stress, destroys the cross-linking of collagen molecules, and increases the level of advanced glycation end products, leading to the decrease of bone strength.²⁶ Therefore, hyperhomocysteinemia may be considered a factor that reduces bone mass and damages bone quality. Drugs that reduce Hcy level and oxidative stress can reduce the risk of fracture in hyperhomocysteinemia patients.²⁴ However, some evidence has reported inconsistent findings that there is no association between elevated Hcy concentration and bone



Table 6 Results of Hcy, HHcy, Cys and Cyss in 36 rats plasma samples in the three groups (NC: normal control, OVX: ovariectomy, OVX + HRS: ovariectomy with hydrogen-rich saline administration)

Group	Hcy ($\mu\text{mol L}^{-1}$)	HHcy ($\mu\text{mol L}^{-1}$)	Cys ($\mu\text{mol L}^{-1}$)	Cyss ($\mu\text{mol L}^{-1}$)
NC	0.62 \pm 0.58	0.021 \pm 0.026	8.37 \pm 3.88	0.31 \pm 0.19
OVX	0.50 \pm 0.10	0.027 \pm 0.022	10.86 \pm 2.64	0.55 \pm 0.14
OVX + HRS	0.58 \pm 0.68	0.011 \pm 0.010	8.88 \pm 3.78	0.36 \pm 0.20

mineral density.²⁷ It has been reported that serum Hcy level in elderly patients with osteoporosis is elevated, but the correlation between Hcy and osteoporosis fracture is not statistically significant.²⁸ This is due to the fact that these literature are based on the total concentration of Hcy. From Fig. 4, 5 and Table 5, we found that the value of Hcy/HHcy (Hcy reduced/oxidized) decreases when OP occurs. It maybe the change of the redox pairs of Hcy/HHcy induces an increase activity of a protease (such as cathepsin K) in osteoclasts, which increase the bone resorption.^{63–65} The Hcy/HHcy increases when osteoporosis improved using the hydrogen water to fight oxidative stress. The present work could provide a more accurate REDOX messenger with Hcy/HHcy to future studies on the mechanism of the relationship between Hcy with bone mineral density and osteoporotic fracture risk.

There were few literature on the relationship of Cys and osteoporosis. Cys is formed from total Hcy and is involved in bone metabolism *via* incorporation into collagen and cysteine protease enzymes. There was a report about a significant association between plasma Cys and bone mineral density. Subjects with low bone mineral density had a significantly lower plasma Cys concentration and a significantly higher recent fracture rate.⁶⁶ It has also reported that cysteine may improve the bone mineral density in the OVX mice.⁶⁷ But these reports were only about total Cys and not studied in detail on the mechanism. There was also no report about Cys/Cyss with OP. In present work, we found that the value of Cys/Cyss decreases when osteoporosis OP occurs from Fig. 4, 5 and Table 5. It indicated that the mechanism of relationship between Cys and OP can be detailedly studied from the aspect of oxidative stress in future study.

4.5 Method limitations

HFCF-UF limitations include the nonspecific binding for some drugs, which may be quantified and overcome.⁵⁰ Fortunately, aminothiol is a kind of small polar compound, and there was no significant nonspecific binding in our study. In addition, there was also no enrichment function from the HFCF-UF device when analyzing drugs at a lower concentration than the instrument detection capability.

In our present work, the ratio of Hcy/HHcy (Hcy reduced/oxidized) and Cys/Cyss (Cys reduced/oxidized) could be suitable biomarkers for oxidative stress was only validated in rats. A rigorous clinical trial in humans would be conduct in our further study. Fortunately, we developed and validated a rapid, reliable and accurate HFCF-UF method which could be used in our further study.

The original purpose of our study was to measure not only Hcy/HHcy (Hcy reduced/oxidized) and Cys/Cyss (Cys reduced/oxidized) but also glutathione (GSH) and its oxidized form (GSSG), which are important indicators of oxidative stress and disease risk. But the method was not well validated for the analysis of GSH and GSSG in spiked plasma samples. This may be explained by the fact that numerous physicochemical factors affect GSH and GSSG stability, including sample pH as well as buffer and extraction reagent composition, which prevents reliable GSH and GSSG estimates.⁴³ Moreover, GSH and GSSG are susceptible to degradation and chemical modifications by proteolytic and phase II metabolic enzymes (*e.g.*, γ -glutamyl-trans peptidases and glutathione-s-transferases) and glutathione reductases that can alter GSH and GSSG concentrations within samples during processing and storage.⁶⁸ Future studies should focus on overcoming these limitations.

5 Conclusions

In the present work, we developed and validated a rapid, reliable and accurate HFCF-UF method for quantifying two reduced form of thiols-homocysteine (Hcy), cysteine (Cys) levels and their respective oxidized compounds, homocystine (HHcy) and cystine (Cyss) in rat plasma simultaneously for the first time. The sample preparation is simplified to a step of 5 min ordinary centrifugation. Without the influence of coprecipitation, strong oxidizing acid, and unprecipitated proteins, the whole operation is performed in a closed system which almost not disturb the redox equilibrium system *in vivo* and the results are more reliable. The method validation parameters complied with FDA guidelines very well. The Hcy/HHcy (Hcy reduced/oxidized) and Cys/Cyss (Cys reduced/oxidized) could be suitable biomarkers for oxidative stress, especially Hcy/HHcy is more sensitive. The developed method provides a valuable tool that may be used to monitor thiol changes in ongoing human clinical developments for diagnostic disease risk evaluation.

Author contributions

Wei-Chong Dong is responsible for paper writing and HPLC-MS/MS method development, Jia-Liang Guo is responsible for animal experiment and statistical research. Xin-Hui Jiang is responsible for and determination of the sample. Lei Xu is responsible for sample collection. Huan Wang and Xiao-yu Ni are responsible for sample preparation and measurement. Ying-Ze Zhang is responsible for animal experimental design and Zhi-Qing Zhang is responsible for data analysis. Ye Jiang is responsible for the method design and HFCF-UF development.



Conflicts of interest

The authors declare no conflict of interest.

Acknowledgements

The work is financially supported by National Natural Science Foundation of China (82002281) and the Natural Science Foundation of Hebei Province (H2021206299). The Natural Science Foundation of Hebei (H2021206054), China Postdoctoral Fund (2021 M701785), and the 14th Five-Year Clinical Medicine Innovation Research Team (2022) also supported this work.

References

- 1 J. Santolini, S. A. Wootton, A. A. Jackson and M. Feelisch, *Curr. Opin. Physiol.*, 2019, **9**, 34–47.
- 2 H. Sies, *Redox Biol.*, 2015, **4**, 180–183.
- 3 X. J. Ren, Y. Zhang, F. Zhang, H. Zhong, J. P. Wang, X. J. Liu, Z. G. Yang and X. Z. Song, *Anal. Chim. Acta*, 2020, **1097**, 245–253.
- 4 Y. H. Yeo and Y. C. Lai, *Curr. Opin. Physiol.*, 2019, **9**, 79–86.
- 5 Z. Daneva, V. E. Laubach and S. K. Sonkusare, *Curr. Opin. Physiol.*, 2019, **9**, 87–93.
- 6 I. Akkawi and H. Zmerly, *Joints*, 2018, **6**, 122–127.
- 7 E. Hernlund, A. Svedbom, M. Ivergard, J. Compston, C. Cooper, J. Stenmark, E. V. McCloskey, B. Jönsson and J. A. Kanis, *Arch. Osteoporos.*, 2013, **8**, 136.
- 8 P. Wang, L. Liu and S. F. Lei, *Clin. Nutr.*, 2021, **40**, 1588–1595.
- 9 D. M. Black and C. J. Rosen, *N. Engl. J. Med.*, 2016, **374**, 254–262.
- 10 N. V. Mohamad, S. Ima-Nirwana and K. Y. Chin, *Endocr., Metab. Immune Disord.: Drug Targets*, 2020, **20**, 1478–1487.
- 11 S. C. Manolagas, *Endocr. Rev.*, 2010, **31**, 266–300.
- 12 G. Bonaccorsi, I. Piva, P. Greco and C. Cervellati, *Indian J. Med. Res.*, 2018, **147**, 341–351.
- 13 W. L. Zhang, Y. Li, Y. Liang, X. P. Yin, C. C. Liu, S. Q. Wang, L. Tian, H. Dong and G. T. Li, *ACS Appl. Mater. Interfaces*, 2019, **11**, 30137–30145.
- 14 B. Li, Y. L. Yu, F. Q. Xiang, S. Y. Zhang and Z. W. Gu, *ACS Appl. Mater. Interfaces*, 2018, **10**, 16282–16290.
- 15 W. H. Watson, J. D. Ritzenthaler, P. Peyrani, T. L. Wiemken, S. Furmanek, A. M. Reyes Vega, T. J. Burke, Y. X. Zheng, J. A. Ramirez and J. Roman, *Free Radical Biol. Med.*, 2019, **143**, 55–61.
- 16 A. C. Enomoto, E. Schneider, T. McKinnon, H. Goldfine and M. A. Levy, *Biomed. Chromatogr.*, 2020, **34**, e4854–e4865.
- 17 S. C. Lu, *Biochim. Biophys. Acta*, 2013, **1830**, 3143–3153.
- 18 L. S. Rallidis, N. Kosmas, T. Rallidi, G. Pavlakis, E. Kiouri and M. Zolindaki, *Coron. Artery Dis.*, 2020, **31**, 152–156.
- 19 K. Han, Q. Lu, W. J. Zhu, T. Z. Wang, Y. Du and L. Bai, *Riv. Eur. Sci. Med. Farmacol.*, 2019, **23**, 9582–9589.
- 20 J. E. Baggott and T. Tamura, *Nutrients*, 2015, **7**, 1108–1118.
- 21 F. Cicchetti, L. S. David, A. Siddu and H. L. Denis, *Neurobiol. Dis.*, 2019, **130**, 104530.
- 22 C. Milanese, C. Payán-Gómez and P. G. Mastroberardino, *Curr. Opin. Physiol.*, 2019, **9**, 73–78.
- 23 N. Tyagi, M. Kandel, C. Munjal, N. Qipshidze, J. C. Vacek, S. B. Pushpakumar, N. Metreveli and S. C. Tyagi, *J. Orthop. Res.*, 2011, **29**, 1511–1516.
- 24 M. Saito and K. Marumo, *Curr. Osteoporos. Rep.*, 2018, **16**, 554–560.
- 25 M. D. Martinis, M. M. Sirufo, C. Nocelli, L. Fontanella and L. Ginaldi, *Int. J. Environ. Res. Public Health*, 2020, **17**, 4260.
- 26 R. Saoji, R. S. Das, M. Desai, A. Pasi, G. Sachdeva, T. K. Das and M. I. Khatkhatay, *Arch. Osteoporos.*, 2018, **13**, 108.
- 27 F. L. Zhao, L. J. Guo, X. F. Wang and Y. K. Zhang, *Arch. Osteoporos.*, 2021, **16**, 4.
- 28 Y. J. Lee, J. Y. Hong, S. C. Kim, J. K. Joo, Y. J. Na and K. S. Lee, *Obstet. Gynecol. Sci.*, 2015, **58**, 46–52.
- 29 B. Bayram, G. Rimbach and J. Frank, *J. Agric. Food Chem.*, 2014, **62**, 402–408.
- 30 R. R. De la Flor St Rèmy, M. Montes-Bayón and A. Sanz-Medel, *Anal. Bioanal. Chem.*, 2003, **377**, 299–305.
- 31 I. Rahman, A. Kode and S. K. Biswas, *Nat. Protoc.*, 2006, **1**, 3159–3165.
- 32 L. Ma, J. He, X. q. Zhang, Y. Cui, J. Y. Gao, X. F. Tang and M. Ding, *RSC Adv.*, 2014, **4**, 58412–58416.
- 33 J. G. Espina, M. Montes-Bayón, E. Blanco-González and A. Sanz-Medel, *Anal. Bioanal. Chem.*, 2015, **407**, 7899–7906.
- 34 A. V. Ivanov, B. P. Luzyanin and A. A. Kubatiev, *Bull. Exp. Biol. Med.*, 2012, **152**, 289–292.
- 35 L. Yuan and J. D. Sharer, *Curr. Protoc. Hum. Genet.*, 2016, **89**, 17.21.1–17.21.10.
- 36 M. Tomaiuolo, G. Vecchione, E. Grandone, N. Cocomazzi, B. Casetta, G. D. Minno and M. Margaglione, *J. Chromatogr. B: Anal. Technol. Biomed. Life Sci.*, 2006, **842**, 64–69.
- 37 A. Zinelli, S. Sotgia, B. Scanu, E. Pisani, M. Sanna, S. Sati, L. Deiana, S. Sengupta and C. Carru, *Talanta*, 2010, **82**, 1281–1285.
- 38 M. Y. Maksimova, A. V. Ivanov, E. D. Virus, V. V. Alexandrin, K. A. Nikiforova, P. O. Bulgakova, F. R. Ochtova, E. T. Suanova, M. A. Piradov and A. A. Kubatiev, *Psychiatr., Neurol., Neurochir.*, 2019, **183**, 105393.
- 39 J. Escobar, Á. Sánchez-Illana, J. Kuligowski, I. Torres-Cuevas, R. Solberg, H. T. Garberg, M. U. Huun, O. D. Saugstad, M. Vento and C. Cháfer-Pericás, *J. Pharm. Biomed. Anal.*, 2016, **123**, 104–112.
- 40 G. Chwatko and E. Bald, *J. Chromatogr. A*, 2002, **949**, 141–151.
- 41 W. Chen, Y. Zhao, T. Seefeldt and X. M. Guan, *J. Pharm. Biomed. Anal.*, 2008, **48**, 1375–1380.
- 42 H. Alwael, D. Connolly, L. Barron and B. Paull, *J. Chromatogr. A*, 2010, **1217**, 3863–3870.
- 43 A. S. Claeson, S. Gouveia-Figueira, H. Stenlund and A. I. Johansson, *J. Chromatogr. B: Anal. Technol. Biomed. Life Sci.*, 2019, **1104**, 67–72.
- 44 A. Forgacsova, J. Galba, J. Mojzisova, P. Mikus, J. Piestansky and A. Kovac, *J. Pharm. Biomed. Anal.*, 2019, **164**, 442–451.
- 45 A. Kamińska, P. Olejarz, K. Borowczyk, R. Głowacki and G. Chwatko, *J. Sep. Sci.*, 2018, **41**, 3241–3249.



46 R. Główacki, J. Stachniuk, K. Borowczyk and H. Jakubowski, *Anal. Bioanal. Chem.*, 2016, **408**, 1935–1941.

47 T. Moore, A. Le, A. K. Niemi, T. Kwan, K. Cusmano-Ozog, G. M. Enns and T. M. Cowan, *J. Chromatogr. B: Anal. Technol. Biomed. Life Sci.*, 2013, **929**, 51–55.

48 R. Rellán-Alvarez, L. E. Hernández, J. Abadía and A. Alvarez-Fernández, *Anal. Biochem.*, 2006, **356**, 254–264.

49 Z. Q. Zhang, W. C. Dong, X. L. Yang, J. F. Zhang, X. H. Jiang, S. J. Jing, H. L. Yang and Y. Jiang, *Ther. Drug Monit.*, 2015, **37**, 776–782.

50 W. K. Li, H. Lin, H. T. Smith and F. L. S. Tse, *J. Chromatogr. B: Anal. Technol. Biomed. Life Sci.*, 2011, **879**, 1927–1933.

51 W. C. Dong, Z. Q. Zhang, X. H. Jiang, Y. G. Sun and Y. Jiang, *Eur. J. Pharm. Sci.*, 2013, **48**, 332–338.

52 J. Zhang and D. G. Musson, *J. Chromatogr. B: Anal. Technol. Biomed. Life Sci.*, 2006, **843**, 47–56.

53 L. Zhang, Z. Q. Zhang, W. C. Dong, S. J. Jing, J. F. Zhang and Y. Jiang, *J. Chromatogr. A*, 2013, **1318**, 265–269.

54 X. Y. Wang, J. L. Gao, C. H. Du, J. An, M. J. Li, H. Y. Ma, L. N. Zhang and Y. Jiang, *Bioanalysis*, 2017, **9**, 173–182.

55 W. C. Dong, J. F. Zhang, Z. L. Hou, X. H. Jiang, F. C. Zhang, H. F. Zhang and Y. Jiang, *Analyst*, 2013, **138**, 7369–7375.

56 J. L. Guo, W. C. Dong, L. Jin, P. C. Wang, Z. Y. Hou and Y. Z. Zhang, *Int. Orthop.*, 2017, **41**, 2119–2128.

57 M. P. Schoenfeld, R. R. Ansari, J. F. Zakrajsek, T. R. Billiar, Y. Toyoda, D. A. Wink and A. Nakao, *Med. Hypotheses*, 2011, **76**, 117–118.

58 C. Fu, D. Xu, C. Y. Wang, Y. Jin, Q. Liu, Q. Meng, K. X. Liu, H. J. Sun and M. Z. Liu, *J. Cell. Physiol.*, 2015, **230**, 2184–2201.

59 W. C. Dong, J. L. Guo, M. Q. Zhao, X. K. Wu, Y. X. Cui, J. Y. Feng, C. X. Zhang, Y. Jiang and Z. Q. Zhang, *Anal. Bioanal. Chem.*, 2021, **413**, 6225–6237.

60 Z. Lin, J. J. Zheng, J. R. Chen, M. M. Chen and S. X. Dong, *Oxid. Med. Cell. Longevity*, 2021, 2098820.

61 Y. X. Zheng, J. D. Ritzenthaler, T. J. Burke, J. Otero, J. Roman and W. H. Watson, *Free Radical Biol. Med.*, 2018, **118**, 13–22.

62 D. P. Jones and Y. L. Liang, Measuring the poise of thiol/disulfide couples *in vivo*, *Free Radical Biol. Med.*, 2009, **47**, 1329–1338.

63 M. A. Gentile, D. Y. Soung, C. Horrell, R. Samadfam, H. Drissi and L. T. Duong, *Bone*, 2014, **66**, 72–81.

64 K. Mukherjee and N. Chattopadhyay, *Biochem. Pharmacol.*, 2016, **117**, 10–19.

65 B. Walia, E. Lingenheld, L. Duong, A. Sanjay and H. Drissi, *Ann. N. Y. Acad. Sci.*, 2018, **1415**, 57–68.

66 M. Baines, M. B. Kredan, A. Davison, G. Higgins, C. West, W. D. Fraser and L. R. Ranganath, *Calcif. Tissue Int.*, 2007, **81**, 450–454.

67 N. R. Han, N. R. Kim, H. M. Kim and H. J. Jeong, *Reprod. Sci.*, 2016, **23**, 670–679.

68 S. G. Lee, J. Yim and Y. Lim, *J. Chromatogr. B: Anal. Technol. Biomed. Life Sci.*, 2016, **1019**, 45–50.

